Chapter 1
Spectroscopy and the Electromagnetic Spectrum

Corey N. Stedwell and Nicolas C. Polfer

1.1 Light and Matter

Electromagnetic radiation exhibits properties of both particles and waves, known as the wave–particle duality. In the wave model, electromagnetic radiation is characterized by its *frequency*, v, *wavelength*, λ, and velocity, c. These three values are related by the relationship

$$c = v\lambda \tag{1.1}$$

The value of c is constant in a given medium (e.g., 2.99×10^8 ms^{-1} in vacuum), while the frequency and wavelength of light are inversely proportional to one another. The SI units for wavelength and frequency are the meter (m) and the hertz (Hz), respectively. Traditionally, spectroscopists also define electromagnetic radiation by the unit *wavenumbers*, defined as

$$\tilde{v} = \lambda^{-1} \tag{1.2}$$

where λ denotes the wavelength in centimeters.

The energy of a photon (quantum of electromagnetic radiation) depends solely on its frequency (or wavelength) and is defined as

$$E = hv = \frac{hc}{\lambda} = hc\tilde{v} \tag{1.3}$$

where h is Planck's constant (6.63×10^{-34} Js) [1]. Note that energy is directly proportional to frequency and wavenumber, and inversely proportional to

C. N. Stedwell (✉) · N. C. Polfer
Department of Chemistry, University of Florida, Gainesville, FL 32611, USA
e-mail: cstedwell@ufl.edu

N. C. Polfer
e-mail: polfer@chem.ufl.edu

Table 1.1 Summary of the frequency, wavenumber, and energy ranges for several regions of the electromagnetic spectrum

Region	Wavelength/m	Wavenumber/cm^{-1}	Energy/eV
Ultraviolet	4.0×10^{-7}–1.0×10^{-8}	2.5×10^{4}–1.0×10^{6}	3.1×10^{0}–1.2×10^{2}
Visible	8.3×10^{-7}–4.0×10^{-7}	1.2×10^{4}–2.5×10^{4}	1.5×10^{0}–3.1×10^{0}
Near-IR	1.5×10^{-6}–8.3×10^{-7}	6.7×10^{3}–1.2×10^{4}	8.3×10^{-1}–1.5×10^{0}
Mid-IR	1.0×10^{-5}–1.5×10^{-6}	1.0×10^{3}–6.7×10^{3}	1.2×10^{-1}–8.3×10^{-1}
Far-IR	1.0×10^{-4}–1.0×10^{-5}	1.0×10^{2}–1.0×10^{3}	1.2×10^{-2}–1.2×10^{-1}
Microwave	1.0×10^{-1}–1.0×10^{-4}	1.0×10^{-1}–1.0×10^{2}	1.2×10^{-5}–1.2×10^{-2}

wavelength. General ranges for frequency, wavelength, and energy limits for several regions of the electromagnetic spectrum are given in Table 1.1.

1.2 The Nature of Light

Visible (vis) light, microwaves, X-rays, and so forth are all different kinds of electromagnetic radiation. Taken collectively, they make up the *electromagnetic spectrum*, depicted in Fig. 1.1.

The electromagnetic spectrum is arbitrarily divided into regions, and it is clear that the familiar, vis portion of the spectrum (i.e., 390–750 nm) constitutes only a small section of the full spectrum. The vis region is flanked by the higher-energy, ultraviolet (UV) and the lower-energy, infrared (IR) and microwave regions. These frequency ranges are the most widely used in spectroscopic measurements, as they can each provide key structural insights into analyte molecules. The microwave
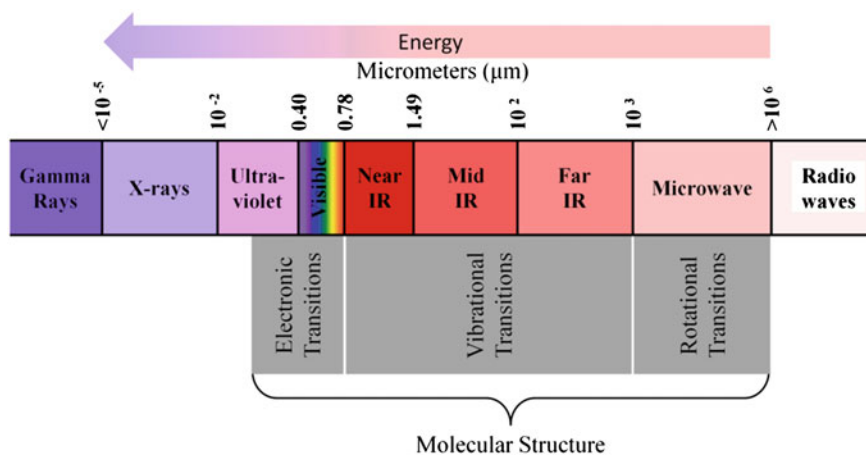

Fig. 1.1 The electromagnetic spectrum covers a continuous range of wavelengths, from low-energy radio waves to gamma (γ) rays at the high-energy end

region of the electromagnetic spectrum is associated with rotational spectroscopy, while the UV and vis portions correspond to molecular electronic transitions. The IR region, which is typically broken into near-, mid-, and far-IR, is utilized in vibrational spectroscopy, as the frequencies of radiation therein correspond to molecular vibrations.

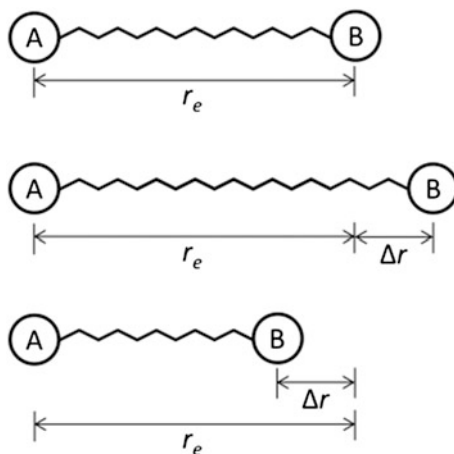## 1.3 Vibrations

1.3.1 Background

There are two general types of molecular vibrations, namely stretching and bending. The stretching frequency of a bond can be approximated by Hooke's law [2, 3]. In this approximation, two atoms and the connecting bond are treated as a simple *harmonic oscillator* composed of two masses (atoms) joined by a spring (a chemical bond). This is illustrated for atoms, labeled A and B, in Fig. 1.2.

These two atoms have some equilibrium distance, r_e, and as the atoms are displaced from their equilibrium distance, they will experience a restoring force, F, that opposes the motion. If we assume that the system behaves according to classical mechanics, the restoring force will be proportional to the displacement from equilibrium distance, Δr, and vary according to Hooke's law

$$F = -k\Delta r \tag{1.4}$$

where k is the *force constant*. At some point, the restoring force will cause the molecular motion to cease, and subsequently, the atoms will begin moving in the opposite direction. This creates a smooth oscillatory motion known as a vibration.

Fig. 1.2 Motions of a diatomic oscillator AB

The frequency of vibration of the system is related to the mass and the force constant of the spring, by

$$v = \frac{1}{2\pi}\sqrt{\frac{k}{\mu}} \tag{1.5}$$

where μ is the *reduced mass* and is defined as

$$\mu = \frac{m_A m_B}{m_A + m_B} \tag{1.6}$$

with m_A and m_B being the mass of atoms A and B, respectively.

In the classical harmonic oscillator, the energy of the vibration is given by

$$E = \frac{1}{2}k\Delta r^2 = hv \tag{1.7}$$

Thus, the energy (or frequency) is dependent on how far one stretches or compresses the spring. In a classical picture, any value of r is possible. If this model were true, a molecule could absorb energy of any wavelength. However, vibrational motion is quantized (it must follow the rules of quantum mechanics), and the only allowed transitions fit the equation

$$E(\mathbf{v}) = \left(\mathbf{v} + \frac{1}{2}\right)hv \tag{1.8}$$

where v is the frequency of the vibration and $\mathbf{v}$ is the *vibrational quantum number* (0, 1, 2, 3, …). The concept of the quantum-mechanical harmonic oscillator potential energy curve is illustrated in Fig. 1.3, indicating the vibrational states.

Note that v does not depend on the value of the quantum number $\mathbf{v}$. Hence, the molecular vibrational frequency is the same in all states, even though the energy E changes with $\mathbf{v}$ in Eq. (1.8). The lowest possible energy level, $\mathbf{v}_0$, resides above the bottom of the energy curve; this difference is known as the *zero-point energy*.

The *gross selection rule* for vibrational transitions stipulates that the electric dipole moment of the molecule must change during the course of a vibration. In other words, the so-called *transition dipole moment*, μ_{fi}, between states i and f must be non-zero. More rigorously,

$$\mu_{fi} = \int \Psi_f^* \hat{\mu} \Psi_i \neq 0 \tag{1.9}$$

where Ψ_i and Ψ_j are wavefunctions describing the ith and jth states, * denotes the complex conjugate of the wavefunction, and $\hat{\mu}$ is the electric dipole moment operator. If the value of this integral is non-zero, then the vibrational mode is said to be *IR active*, meaning that the transition is allowed and hence observed. A vibrational mode is said to be *IR inactive* if the dipole moment of the molecule does not change during the vibration, as for instance in a homonuclear diatomic molecular vibration.

Fig. 1.3 Quantum-mechanical harmonic oscillator indicating allowable energy levels
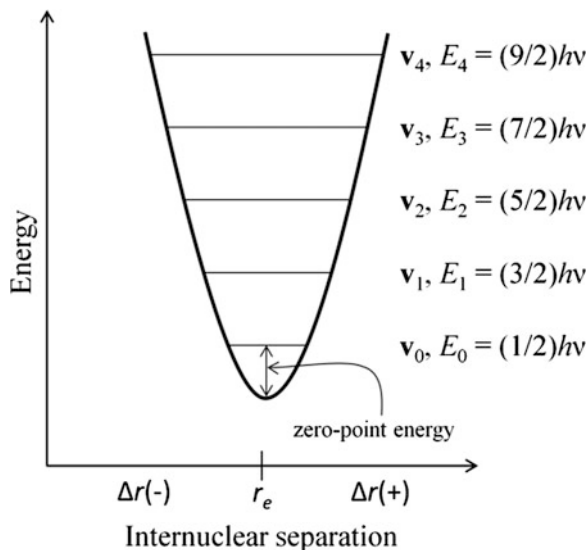
The *specific selection rule* for the harmonic oscillator limits changes in the vibrational quantum number to $\Delta \mathbf{v} = \pm 1$. Substituting any state $\mathbf{v}$ and $\mathbf{v} + 1$ in Eq. (1.8), we can see that the energy difference between any two states is

$$\frac{\Delta E}{hc} = \frac{v}{c} = \tilde{v} \qquad (1.10)$$

(i.e., the energy of the vibrational transition in wavenumbers is the same as the molecule's vibrational frequency).

In reality, molecules are not perfect harmonic oscillators. In other words, the variation in the potential energy of the system with internuclear separation is not perfectly symmetric, but rather tends to have a skewed appearance, similar to that of the *Morse potential*, as shown in Fig. 1.4. This type of potential energy dependence describes the behavior of an *anharmonic oscillator*, where the spacing between subsequent energy levels is reduced for higher-energy states [4].

Similar to the harmonic oscillator, Schrödinger's equation can be solved for the Morse potential, resulting in the following expression for energy states

$$E = hv \left[\left(\mathbf{v} + \frac{1}{2} \right) - x_e \left(\mathbf{v} + \frac{1}{2} \right)^2 + \cdots \right] \qquad (1.11)$$

where x_e is called the *anharmonicity constant*. In general, higher-order terms in Eq. (1.11) are usually small and are routinely omitted. Energy-state separation between any two successive states can then be given by

$$\Delta E = hv[1 - 2x_e(\mathbf{v} + 1)] \qquad (1.12)$$
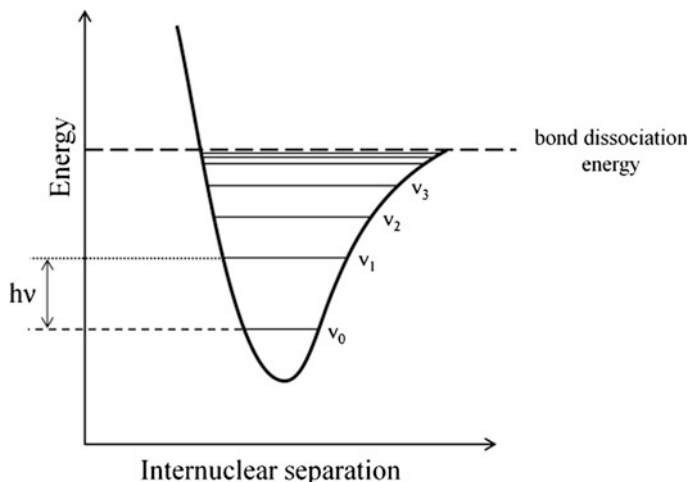
Fig. 1.4 Potential energy curve of an anharmonic oscillator (Morse potential). Energy-level separations decrease as **v** increases

where **v** is taken as the vibrational quantum number for the lower-energy state. In most cases, x_e is a positive number, so that the separation of successive states becomes progressively smaller as **v** increases.

The frequency recorded for a molecular vibration by IR spectroscopy corresponds to the energy difference between two vibrational states. The transition between **v** = 0 and **v** = 1 is known as the *vibrational fundamental*. For the IR absorption corresponding to the fundamental transition, we can see from Eq. (1.12) that the energy of the observed transition will be

$$\Delta E = hv[1 - 2x_e] \tag{1.13}$$

At the limit when $x_e \rightarrow 0$, one can easily see that harmonic oscillator behavior is restored (i.e., $\Delta E = hv$), and the observed vibrational frequency is the same as the molecular vibrational frequency.

Thus far, we have discussed harmonic and anharmonic representations of a diatomic molecule. Let us now consider the molecular motions of a polyatomic molecule with *n* atoms. The motions of each atom can be resolved into components along the three directions in the Cartesian coordinate system. Therefore, any molecule composed of *n* atoms has 3*n degrees of freedom*. These 3*n* degrees of freedom encompass vibrations, rotations, and translations. The vibrational motions of atoms can be expressed as fundamental vibrational modes of the entire molecule, known as *normal modes*. The number of vibrational modes will be 3*n* minus the number of non-vibrational modes. For linear molecules, which have three translational and two rotational motions, they possess 3*n*-5 normal modes. In contrast, nonlinear molecules possess three rotational and three translational motions and hence have 3*n*-6 vibrational modes. Apart from the general

classification of stretching and bending modes, the bending modes can be further specified as scissoring, rocking, wagging, and twisting vibrations. The different kinds of IR-active vibrations are illustrated in Fig. 1.5 for the example of a CH_2 moiety.

1.3.2 Biomolecular Vibrations

As can be visualized from Fig. 1.5, along with the total number of molecular normal modes, it is easy to see that biomolecules can contain a large number of IR-active vibrational modes. Since most biomolecules contain a permanent dipole moment and have low symmetry, most normal modes are IR active. The stronger, measurable vibrational modes can lend key insights into molecular structure (i.e.,

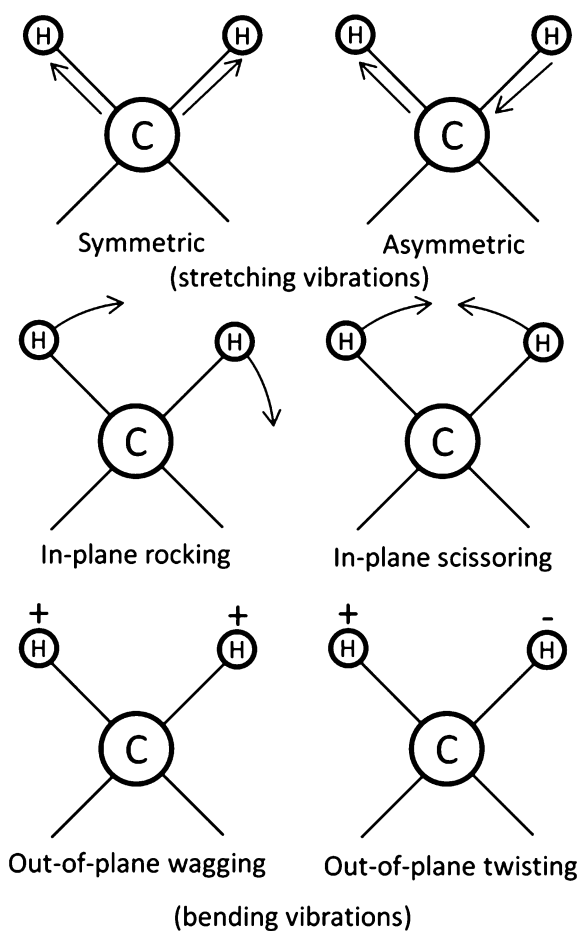**Fig. 1.5** Types of molecular vibrational motions shown for a CH_2 moiety

Symmetric   Asymmetric
(stretching vibrations)

In-plane rocking   In-plane scissoring

Out-of-plane wagging   Out-of-plane twisting

(bending vibrations)

Table 1.2 Vibrational ranges for common biomolecular chemical moieties

Description	Frequency/cm^{-1}
P-OH stretch/P-OH wag	920–1,080
Amide NH bending	1,475–1,525
Amide CO stretch	1,675–1,725
Carboxylic acid CO stretch	1,725–1,775
Symmetric NH$_2$ stretch	3,350–3,400
Asymmetric NH$_2$ stretch	3,400–3,450
Amide NH stretch	3,300–3,500
Indole/Imidazole NH stretch	3,480–3,520
Carboxylic acid OH stretch	3,540–3,600
Alcohol OH stretch	3,600–3,675
Phosphate OH stretch	3,650–3,700

presence of chemical moieties) and typically reside within known frequency ranges. Some of the more biologically relevant vibrational modes are summarized in Table 1.2. With some of these vibrations lying in diagnostic regions of the electromagnetic spectrum, one can easily see why the IR spectrum is such a powerful tool in determining the chemical structures of analytes. Many of the remaining IR modes are either weak, and are hence challenging to measure, or located in congested regions of the IR spectrum, and are therefore difficult to unambiguously assign.

In the event that an experimental band assignment to a particular vibrational mode is ambiguous, chemical labeling strategies can be employed to deconvolute the IR spectrum. One such technique is *isotope labeling*, wherein an atom is selectively replaced with a heavier isotope of the same atom. For example, site-specific information can be obtained on an amide CO stretching vibration by replacing the ^{12}C with a ^{13}C.

Let us consider a diatomic CO molecule in the harmonic oscillator approximation. While this simplistic view is not an accurate representation of an amide moiety with full molecular considerations, the principle can be illustrated by looking at the vibrational frequency shift due to isotopic labeling of the carbon atom in the diatomic CO. Recall the frequency of a vibration given by Eq. (1.5), where the frequency is a function of the reduced mass of the system. When an atom is labeled with a heavier isotope, the reduced mass of the system is increased. Due to the inverse relationship between vibrational frequency and reduced mass, it is apparent that the vibrational frequency should be reduced upon an increase in the mass of the system (refer to Eq. 1.6). To illustrate this, the difference in frequency upon isotopic labeling is given by

$$\Delta v = v_{^{12}CO} - v_{^{13}CO} = \frac{\sqrt{k}}{2\pi}\left(\frac{1}{\sqrt{\mu_{^{12}CO}}} - \frac{1}{\sqrt{\mu_{^{13}CO}}}\right) \tag{1.14}$$

where the frequencies and reduced masses of interest are denoted by the respective carbon isotope labels (i.e., 12 or 13). The force constant of CO has been

experimentally determined to be $k = 1,854$ N/m. Hence, a quick calculation yields a frequency redshift of $\Delta v = 48$ cm^{-1} upon ^{13}C labeling of a CO diatomic. Note that this frequency shift is the maximum possible frequency shift for a single oscillator. In larger molecules, a normal mode often involves oscillation of multiple subentities of the molecule. Due to the larger overall reduced mass, the effect of the isotopic substitution is markedly diminished, thus lessening the observed frequency shift.

1.4 Electronic Transitions

1.4.1 Background

The interaction between UV and vis light with matter generally entails an electronic transition (i.e., promotion of electrons from the electronic ground state [S_0] to a higher-energy state [e.g., S_1]) [5]. For a molecule, A, this process can be visualized by

$$A + hv \rightarrow A^* \tag{1.15}$$

where v is the frequency of radiation and A* represents an excited electronic state of A. Molecules containing π-electrons or non-bonding electrons can absorb energy from an UV or vis light source, which promotes electrons to higher-energy antibonding molecular orbitals. A schematic representation of the different types of transitions is given in Fig. 1.6. In general, there are three types of transitions; $\sigma \rightarrow \sigma^*$ transitions usually occur in the vacuum UV (i.e., <200 nm) and will not be considered here. The lower-energy $n \rightarrow \pi^*$ and $\pi \rightarrow \pi^*$, read "n to π star transition" and "π to π star transition," typically reside in the 200 nm < λ < 750 nm (UV–vis) region. The lowest energy transition is a promotion from the highest occupied molecular orbital (*HOMO*) to the lowest unoccupied molecular orbital (*LUMO*). For the example given in Fig. 1.6, the nonbonding orbital is the highest energy orbital that contains an electron and the π^* antibonding orbital is the lowest energy unoccupied orbital, which gives rise to the $n \rightarrow \pi^*$ HOMO–LUMO transition.

Another important aspect of electronic transitions is the fast timescale on which the absorption occurs (e.g., 10^{-15}–10^{-18} s). In general, electronic transitions occur several orders of magnitude faster than atomic vibrations ($\sim 10^{-13}$ s). According to the *Franck–Condon principle*, electronic transitions are considered instantaneous when compared to nuclear motions. In other words, absorptions, as shown on a potential energy curve, are essentially *vertical transitions* and the nuclear coordinates remain effectively unchanged during electronic excitations (see Fig. 1.7). Radiation of frequency v can be absorbed if the energy difference hv corresponds to the energy difference between a quantized energy level in the excited state and a quantized energy level in the ground state.
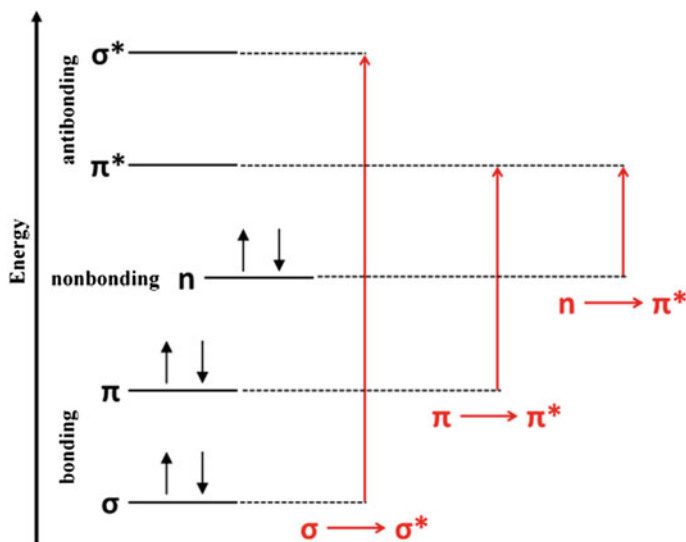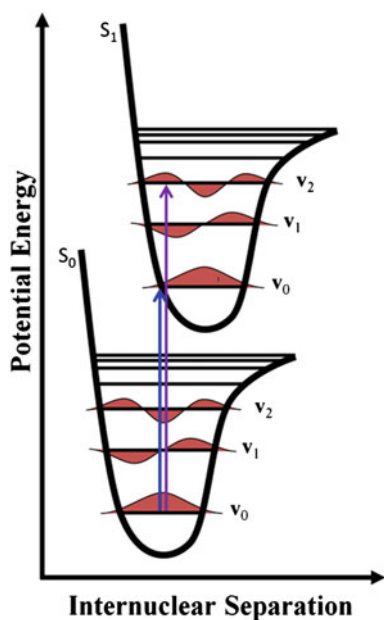
Fig. 1.6 Energy diagram depicting common electronic transitions

Fig. 1.7 Electronic
transitions from the
vibrational ground state of S_0
to different vibrational levels
of S_1 (i.e., v_0 and v_2)

Since the electronic-state wavefunctions are orthogonal to one another (i.e., the overlap integral is equal to zero), the probability of an electronic transition is proportional to the square of the overlap integral between the ground-state

vibrational wavefunction and the excited-state vibrational wavefunction. The vibrational-state overlap integral is referred to as the *Franck–Condon factor* and governs the strength of electronic transitions based on the compatibility of the nuclear coordinates in the initial and final states of the transition. Hence, the probability of a transition is significantly reduced if the initial and final states correspond greatly to differing interatomic distances, as the nuclei would be required to undergo significant spatial changes accompanying the electronic transition. For the example illustrated in Fig. 1.7, one would expect the vibronic transition $\mathbf{v}_0 \rightarrow \mathbf{v}_2$ (purple arrow) to be stronger than the origin band $\mathbf{v}_0 \rightarrow \mathbf{v}_0$ (blue arrow), based on greater overlap, and a larger Franck–Condon factor, in the ground- and excited-state wavefunctions in the former case. For a more detailed discussion of the Franck–Condon principle, the reader is referred to relevant literature [3, 6].

1.4.2 Applications to Biomolecular Systems

For UV–vis spectroscopy to be applicable to biomolecular systems, a key requirement must be met. The system must contain a UV chromophore capable of absorbing photons in the UV–vis frequency range. For biological systems, this requirement is met in numerous cases. For instance, several amino acids act as UV chromophores (e.g., histidine, tyrosine, and tryptophan). Therefore, most systems (isolated amino acids, peptides, and proteins) that include these subunits will exhibit adequate UV absorption cross-sections. In addition, the peptide bond itself has the ability to absorb UV photons in the 190–230 nm range. On the other hand, saccharides do not exhibit absorption in the typical UV–vis range. Hence, such molecules must be subjected to chemical derivatization to be detected by UV spectroscopy. Since UV–vis spectra tend to contain superpositions of various vibronic transitions, and contributions from various conformers, absorption peaks tend to be broad and a limited amount of structural information can be obtained from these measurements. Some steps can be taken to sharpen the electronic transition bands and obtain structural (even conformer specific) information, a point that will be discussed further in Sect. 1.6.

1.5 Absorption Spectroscopy

To this point, we have discussed various types of transitions, both vibrational and electronic. Let us now turn our attention to the practical aspects of measuring the aforementioned transitions. First, we will consider the traditional absorption spectroscopy experiment. Absorption of photons by a species is governed by the Beer–Lambert law [5]

$$-\log(T) = A = \varepsilon l c \tag{1.16}$$

where T is the transmittance of light through the substance, A is the absorbance, ε is the molar absorptivity coefficient, l is the distance of interaction (i.e., the path length), and c is the molar concentration of the absorbing species. A simple measurement of T can be performed by measuring

$$T = \frac{I}{I_0} \tag{1.17}$$

where I and I_0 are the intensities of the incident and transmitted light, respectively. The UV–vis absorption spectroscopy experiment is illustrated in Fig. 1.8. Light from a light source is passed through a monochromator. The monochromatic light is split, passed through a blank absorption cell (i.e., to measure I_0), and passed through the sample (i.e., to measure I). A detector records the intensities of the respective signals, and a ratio of the two intensities is a direct measurement of T.

As can be seen in Fig. 1.8, a traditional absorption measurement is based on a simple setup, which, nonetheless, provides powerful measurements. From Eqs. 1.16 and 1.17, it is immediately apparent where the traditional absorption measurement becomes difficult. For this experiment to be successful, there must be a **measureable** difference between I and I_0. This becomes challenging when the values of ε, l, or c are small. Naturally, the value of l depends on the experimental setup; however, for practical reasons (e.g., instrumental cost, space requirements), it is best that the path length remains at a reasonable value. The value of c is sample dependent (e.g., sample availability, solubility), while the value of ε is inherent to the absorbing species.

In many physical chemistry experiments, the molar concentration of the absorbing species is extremely low. For instance, reactive species with short lifetimes may not exist in measurable quantities. In addition, absorption measurements are often ill-suited for the detection of gas-phase molecules, particularly ions in a mass spectrometer. To illustrate the limitations of the traditional absorption spectroscopy experiment, we consider the amino acid tryptophan in its ionized form. Tryptophan exhibits a moderate UV photoabsorption at 280 nm, with a molar absorptivity coefficient $\varepsilon = 5{,}690\ \mathrm{M^{-1}cm^{-1}}$. If we reasonably assume an absorption path length $l = 1$ cm and a detection efficiency (I/I_0) of 0.1 %, then one can derive (from Eqs. 1.16 and 1.17) that the required concentration of tryptophan would need to be approximately 75 nM. This corresponds
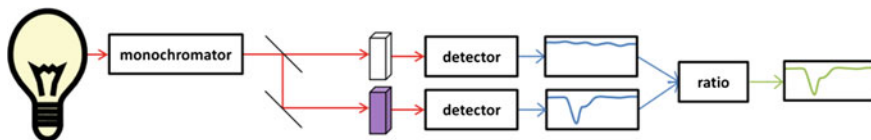

Fig. 1.8 Block diagram of a typical absorption spectroscopy measurement

to $\sim 4.6 \times 10^{13}$ tryptophan ions per mL of probed solution, which contrasts to a maximum of $\sim 10^7$ ions that can typically be trapped in a mass spectrometer. The vastly lower concentrations of ions in mass spectrometers clearly preclude spectroscopic interrogation via conventional absorption detection schemes. One must therefore turn to more sensitive spectroscopic methods—referred to as "consequence" or "action" spectroscopy—to enable these experiments.

1.6 Consequence Spectroscopy

1.6.1 Background

As illustrated in the previous section, the direct measurement of photon absorption imposes limitations that hinder experiments with low number densities of absorbing species. *Consequence* (or "action") *spectroscopy*, where it is not the absorption of photons that is detected, but rather the consequence of the absorption that is detected, overcomes these limitations. Consequence spectroscopic techniques are predicated in the fact that a measurable, physical property of the analyte molecules changes as a direct result of photon absorption. For the purposes of this book, as it relates to biomolecular ions, the mass, or *mass-to-charge (m/z) ratio*, is the physical property most often utilized for such measurements, as the *m/z* ratio is readily attained by a mass spectrometer (discussed further in Chap. 3). To illustrate, Fig. 1.9 schematically depicts the measurement of a consequence absorption spectrum via measurement of the mass spectrum of an analyte molecule. Analyte ions, of a given *m/z* ratio, are subjected to irradiation by a tunable light source (refer to Chap. 2) at discrete frequency steps, and changes in the *m/z* ratio are measured at each frequency step (Fig. 1.9 left). The *m/z* ratio of an analyte changes when a sufficient number of photons have been absorbed to cause photodissociation (i.e., generation of photofragments). As the frequency of the incident light is changed, the number of absorbed photons per ion, and thus the extent of photodissociation, changes according to the absorption cross-section at the given frequency. A consequence absorption spectrum can then be constructed by plotting the yield of photodissociation as a function of radiation frequency (Fig. 1.9 right). In this spectrum, molecular absorptions are manifested as an enhanced photodissociation yield, as opposed to no, or negligible, photodissociation at non-resonant frequencies.

Since this technique relies on the detection of ions with differing *m/z* values, rather than detection of the number of photons absorbed by an analyte, consequence spectroscopy techniques provide an indirect measurement of the absorption spectrum. Due to the indirect nature of the experiment, one must take caution not to overinterpret the results, as a number of assumptions are made. However, due to the sensitivity of modern-day mass spectrometers, the sensitivity of the measurement is telling. A mere, few hundred analyte molecules are sufficient, in stark
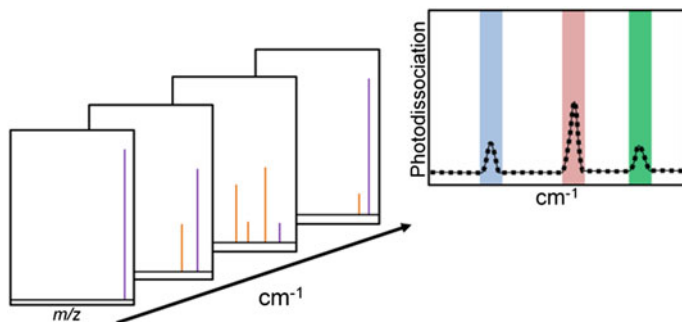
Fig. 1.9 Methodology of a photodissociation consequence spectroscopy measurement. Precursor ions (purple) photodissociate to fragments (orange) upon resonant photon absorption. Absorption bands are highlighted for illustrative purposes

contrast to the macroscopic number of analyte molecules required for a traditional absorption measurement.

Over the past few decades, a number of consequence spectroscopy techniques have been applied to analyze biomolecular ions, including (1) infrared multiple-photon dissociation (IRMPD) spectroscopy, (2) ultraviolet photodissociation (UVPD) spectroscopy, (3) infrared–ultraviolet (IR–UV) ion dip spectroscopy, (4) IR predissociation spectroscopy, and (5) photoelectron spectroscopy. The first four of these will be elaborated on with some detail. Note that IR–UV ion dip spectroscopy is an extension of UVPD, as it allows the measurement of IR spectra of UV-selected conformers. The conceptual approaches to IRMPD, IR predissociation, and IR–UV ion spectroscopy are summarized in Fig. 1.10, and each method will be discussed in turn below.

1.6.2 Infrared Multiple-Photon Dissociation Spectroscopy

IRMPD spectroscopy is easily implemented in commercially available trapping mass spectrometers. In terms of instrumentation requirements, IRMPD spectroscopy is the least technically demanding; however, this approach also results in the lowest resolution consequence IR spectra of the techniques that will be discussed. IRMPD requires only a trapping mass spectrometer and a tunable IR light source that can provide sufficient photon flux.

Generally, room-temperature ions are trapped for an extended period of time (i.e., seconds) and are irradiated with the output of a tunable IR photon source. The IRMPD process requires the absorption of multiple IR photons to surpass the dissociation threshold, visualized by a white dashed line in Fig. 1.10 left, of the analyte. When the IR photons are in resonance with the fundamental transition (i.e., $\mathbf{v}_0 \rightarrow \mathbf{v}_1$) of a vibrational mode, a photon is efficiently absorbed by the ions. However, subsequent transitions (e.g., $\mathbf{v}_1 \rightarrow \mathbf{v}_2$) are not resonant with the photon
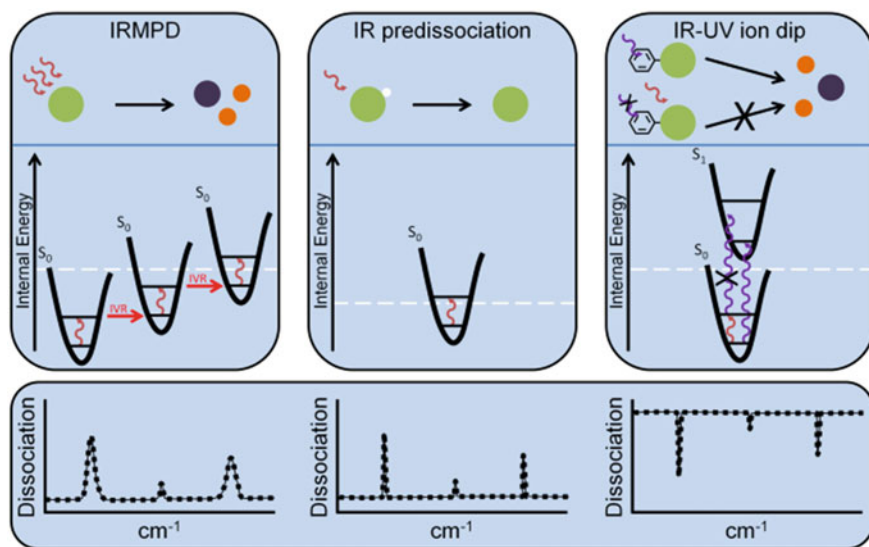
Fig. 1.10 Summary of infrared consequence spectroscopy techniques. Figure adapted from [7]

source, as the spacing between vibrational modes is reduced, due to anharmonicity. This "anharmonic bottleneck" prohibits dissociation via the so-called ladder-climbing process (i.e., $v_0 \rightarrow v_1 \rightarrow v_2 \rightarrow \ldots \rightarrow$ dissociation). On the other hand, if other normal modes couple with the initially absorbing normal mode, energy can be dispersed throughout the molecule by *internal vibrational redistribution* (IVR). Through IVR, energy is quickly (i.e., ps timescale) dissipated throughout the bath of normal modes of the molecule, effectively depopulating the v_1 state and returning the molecule to the vibrational ground state. The absorption of a subsequent photon at the fundamental frequency is then possible, again followed by dissipation of the energy throughout the molecule. This cycle is repeated many times (i.e., tens to hundreds), in the process raising the internal energy of the molecule to exceed the dissociation threshold of the molecule, and thus induces photodissociation into one, or multiple, fragmentation channels.

The IRMPD technique is based on a slow, sequential absorption of photons, causing a gradual increase in the internal energy (i.e., heating) of the ions. Therefore, in most cases, ions dissociate by the lowest energy dissociation threshold, such as the loss of a labile chemical moiety. In other words, higher-energy dissociation pathways are typically not accessible, due to the rapid randomization of energy that occurs via IVR. Moreover, while a particular chemical bond or moiety resonantly absorbs the photon energy, this group may not dissociate in the process, but rather other, more labile groups are involved in covalent-bond cleavage. The extent of photodissociation by IRMPD, or IRMPD yield, is quantified by

$$\text{IRMPD yield} = \frac{\sum (\text{photofragments})}{\sum (\text{precursor} + \text{photofragments})} \qquad (1.18)$$

or

$$\text{IRMPD yield} = -\ln\left(1 - \frac{\sum (\text{photofragments})}{\sum (\text{precursor} + \text{photofragments})}\right) \qquad (1.19)$$

where Σ represents the sum of the integral intensities of the respective ion signals. Given that the IRMPD yield is limited by the initial ion population of the precursor ion that is irradiated, the yield is expected to follow pseudo-first-order kinetics. In this sense, the logarithmic yield (Eq. 1.19) gives a better approximation of the relative yields, even if the linear approximation for yield (Eq. 1.18) gives numerically comparable results in cases where the IRMPD yield is low. In reality, IRMPD band intensities are affected by nonlinear processes, and hence, spectral intensities are often (slightly) distorted when compared to linear absorption spectra.

Due to the thermal distribution of the probed ion population, multiple conformers (e.g., rotamers) of the analyte ions are usually present, each with a slightly different absorption spectrum. Measured vibrational features in an IRMPD spectrum result from a superposition of multiple conformers, accounting for significant broadening (>15 cm^{-1}). An additional broadening effect arises from ion heating during multiple-photon absorption, as hotter ions have redshifted and broader absorption bands. In summary, the band-broadening effects in IRMPD are a result of both the conformational envelope (accessible at a particular temperature) prior to laser irradiation and the anharmonic effects (i.e., redshifting, broadening) during laser excitation. IRMPD spectroscopy is often well positioned to address questions on the chemical structures of ions, such as confirming the presence (or absence) of chemical moieties in analytes. However, the technique is less suitable to interrogate gas-phase conformations, for which other consequence spectroscopy techniques, which probe cold, conformationally restricted ions, are necessary.

1.6.3 Ultraviolet Photodissociation Spectroscopy

Due to the higher photon energy in the UV region of the electromagnetic spectrum, absorption of a single is generally sufficient to overcome the dissociation threshold. Photodissociation can take place by a number of routes, and the three most common pathways will be briefly discussed. In the highest energy mechanism, the UV photon absorption causes a *vibronic transition* (i.e., a simultaneous change in electronic and vibrational states) from the electronic ground state (S_0) to a highly excited, unbound vibrational level (i.e., above the dissociation threshold) in the electronic excited state, S_1. Promotion to a highly excited vibrational state, beyond the dissociation threshold of S_1, directly results in dissociation; this is shown in

Fig. 1.11 (left). The second mechanism differs only in that dissociation proceeds from the ground electronic state, following an *internal conversion* (i.e., electronic energy is converted into vibrational energy) from the electronically excited state. This can occur by

a. internal conversion directly to a highly excited vibrational state (i.e., above the dissociation threshold) of S_0
b. internal conversion to S_1 v_0, followed by relaxation to a highly excited vibrational state of S_0

and is shown schematically in Fig. 1.11 (center). The third mechanism proceeds via a potential energy curve crossing to a *dissociative state* (DS), which has no, or only a shallow potential energy minimum, hence causing dissociation (Fig. 1.11 right). This results in so-called predissociation or dissociation below normal dissociation thresholds. Electronically excited molecules may also be deexcited, without undergoing photodissociation, by the emission of a photon (i.e., *fluorescence*) or emission of an electron, depending on the energy of the incoming photon, and the charge state and polarity of the ion.

Naturally, UVPD experiments require a coupled tunable UV light source and a trapping mass spectrometer. A UVPD spectrum is measured by monitoring the photodissociation yield as a function of incident UV photon frequency. The relatively high-energy nature of the photons in the UV region permits single-photon (i.e., linear) dissociation. While structural information can be obtained from the electronic spectrum of a room-temperature ion, UVPD spectroscopy tends to result in broader spectral features, due to the multitude of available vibronic transitions
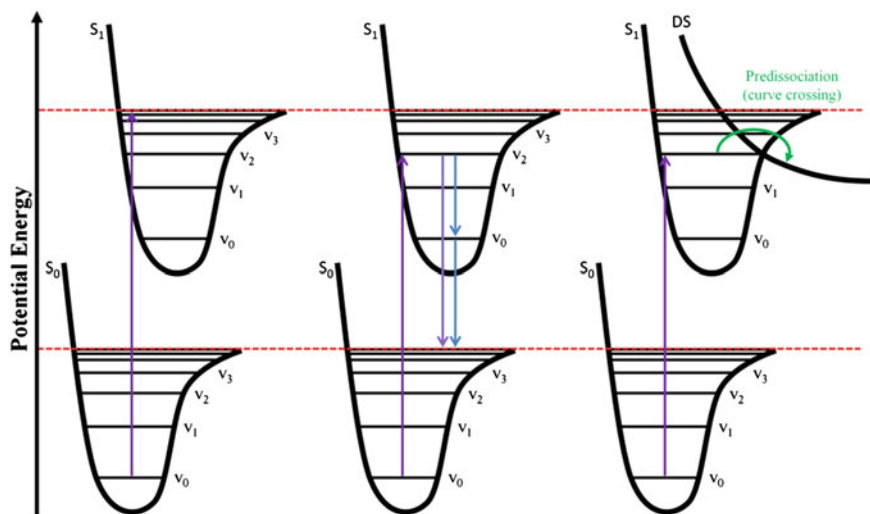

Fig. 1.11 Three potential dissociation mechanisms upon absorption of a UV photon. Dissociation thresholds are indicated via red, dashed lines

that are available. Similar to IRMPD spectroscopy, UVPD spectroscopy on room-temperature ions is more suitable for elucidating chemical structures, as opposed to characterizing conformations.

1.6.4 Infrared–Ultraviolet Ion Dip Spectroscopy

To obtain higher-resolution IR spectra than is possible by UVPD spectroscopy, a key detail must be addressed—the internal energy of the analyte molecules must be decreased to reduce conformational inhomogeneity. High-resolution UV spectra can be collected on cryogenically cooled ions, where sharp transitions correspond to origin and vibronic bands from a population of gas-phase conformers. In order to assign structures to specific UV transitions, it is useful to record the corresponding IR spectra. In IR–UV *ion dip spectroscopy*, conformer-specific IR absorption spectra can be collected by employing a two-laser photo-dissociation scheme.

Trapped ions are cooled to cryogenic temperatures prior to interrogation by IR–UV spectroscopy. In addition, IR–UV requires the use of a pulsed UV light source to photodissociate specific molecular conformers trapped within a mass spectrometer. Since the electronic (UV) transitions are intimately coupled with molecular structure, any two conformers will have slightly differing UV absorptions. The premise of the technique rests on the assumption that a particular UV transition is selective for a specific gas-phase conformation. As is implied, this technique is only applicable to analyte molecules that contain a chromophore capable of absorbing UV photons.

To obtain conformer-specific IR spectra, the UV light source is fixed to a unique UV transition, causing constant photodissociation of the selected conformer. Meanwhile, a tunable, pulsed IR light source is scanned to probe the analyte molecules. If the IR pulse precedes the UV pulse (e.g., by approximately 100 ns), and the IR frequency is in resonance with a $\mathbf{v}_0 \rightarrow \mathbf{v}_1$ vibrational transition of the conformer, an IR photon is absorbed, effectively depleting the ground vibrational state ($S_0 \, \mathbf{v}_0$). In a population of ions, a significant depletion of the ground vibrational state means fewer analyte molecules are in resonance with the UV photon frequency, therefore reducing the amount of measured UVPD (i.e., a "dip" in measured UV photofragmentation yield). In other words, as the frequency of the IR photons is scanned, each dip in the measured UV dissociation corresponds to a different vibrational transition in the molecular conformer being probed by the UV laser. This is visualized graphically in Fig. 1.10 (right). The IR spectrum can be recorded for multiple UV transitions, each potentially corresponding to a different molecular conformer.

IR–UV ion dip spectroscopy is the most sophisticated of the techniques mentioned here. In addition to the mass spectrometer and a cryogenic cooling apparatus, two light sources are required (UV and IR), both of which must be tunable and pulsed. The utility of these types of experiments can be witnessed in the high-

resolution, conformer-specific absorption spectra that are generated (illustrated further in Chap. 4).

1.6.5 Infrared Predissociation Spectroscopy

Another spectroscopic technique that utilizes cold ions is IR *predissociation spectroscopy*, which uses a "messenger" or "tag" species (e.g., Ar, He, H_2) to report on photon absorption and requires that analyte molecules be cooled to cryogenic temperatures so that the messenger species can bind non-covalently prior to laser irradiation. A careful choice of tag species ensures that (1) the absorption bands of the analyte are not perturbed significantly by the presence of the tag and (2) the analyte molecules are sufficiently cold prior to binding, due to the low binding energy between the analyte and tag molecules. Cryogenically cooled analyte molecules have limited internal energy, reducing the number of possible conformations, and hence the spectral complexity. In addition, the low binding energy between the tag and analyte ensures that a single photon causes photodissociation, due to the dramatically reduced dissociation energy threshold (see Fig. 1.10 center). The linearity of this method also allows for the direct comparison of experimental results with *ab initio* electronic structure calculations, which are heavily relied upon to deduce structural information from experimental data.

As one may surmise, IR predissociation spectroscopy is more technically demanding than IRMPD spectroscopy, as in addition to a tunable IR light source and a trapping mass spectrometer, a means is required to cool analyte molecules to cryogenic temperatures. However, significantly higher resolution can be obtained, with feature bandwidths circa a few cm^{-1}. In addition, the predictable nature of the photodissociation channels (i.e., the loss of the tag molecule) allows the experiment to be multiplexed. In contrast to IRMPD and IR–UV ion dip spectroscopy, where numerous photofragments can be generated, predissociation generally results in the loss of a single tag molecule without subsequent dissociation. If overlaps in analyte *m/z* do not occur, in principle, the absorption spectra of several molecules can be measured simultaneously, dramatically increasing data collection efficiency (discussed further in Chap. 4).

References

1. Lide DR (2011) CRC handbook of chemistry and physics: a ready-reference book of chemical and physical data. CRC Press, Boca Raton
2. Giancoli D (2005) Physics: principles with applications. Upper Saddle River, Pearson/Prentice Hall
3. Atkins P, de Paula J (2006) Physical chemistry, 8th edn. W.H. Freeman, New York
4. Carter R (1998) Molecular symmetry and group theory. J. Wiley, New York

5. Harris D (2007) Quantitative chemical analysis. W.H. Freeman and Co, New York
6. Laidler K (1987) Chemical kinetics. Harper & Row, New York
7. Stedwell CN, Galindo JF, Roitberg AE, Polfer NC (2013) Structures of biomolecular ions in the gas phase probed by infrared light sources. Ann. Rev. Anal. Chem. 2013. 6:267–285.